



HAL
open science

Design of self-dessicating binders using calcium sulfoaluminate cement: influence of the cement composition and sulfate source

Céline Cau Dit Coumes, Oriane Farcy, Pascal Antonucci, Jean-Baptiste Champenois, David Lambertin, Adel Mesbah

► To cite this version:

Céline Cau Dit Coumes, Oriane Farcy, Pascal Antonucci, Jean-Baptiste Champenois, David Lambertin, et al.. Design of self-dessicating binders using calcium sulfoaluminate cement: influence of the cement composition and sulfate source. *Advances in Cement Research*, 2019, 31 (4), pp.178-194. 10.1680/jadcr.18.00100 . cea-02339868

HAL Id: cea-02339868

<https://cea.hal.science/cea-02339868>

Submitted on 5 Nov 2019

HAL is a multi-disciplinary open access archive for the deposit and dissemination of scientific research documents, whether they are published or not. The documents may come from teaching and research institutions in France or abroad, or from public or private research centers.

L'archive ouverte pluridisciplinaire **HAL**, est destinée au dépôt et à la diffusion de documents scientifiques de niveau recherche, publiés ou non, émanant des établissements d'enseignement et de recherche français ou étrangers, des laboratoires publics ou privés.

**Design of self-dessicating binders using calcium sulfoaluminate cement:
influence of the cement composition and sulfate source**

Céline Cau Dit Coumes^{a*}, Oriane Farcy^a, Pascal Antonucci^a, Jean-Bapiste Champenois^a,
David Lambertin^a, Adel Mesbah^b

^aCEA, DEN, Univ. Montpellier, DE2D, SEAD, LCBC, F-30207 Bagnols-sur-Cèze cedex,
France

^b ICSM, UMR 5257 CNRS - CEA – ENSCM – Université de Montpellier, Site de Marcoule -
Bât 426, BP 17171, 30207 Bagnols/Cèze, France

* Corresponding author

Tel.: +33 4 66 39 74 50

e-mail address : celine.cau-dit-coumes@cea.fr

Keywords: sulfate-based cement, hydrated cement, thermodynamics

Abstract

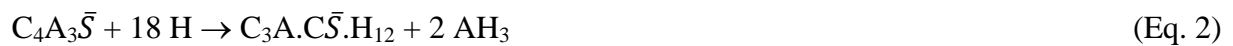
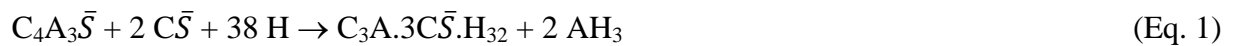
Calcium sulfoaluminate (CSA) cements with a high ye'elimite content are of interest to produce self-desiccating binders. This work investigates the influence of the cement composition and calcium sulfate source on the content of water bound by hydration, with the future goal of designing non-expansive materials with dry internal environments. A thermodynamic approach is first carried out. Ten cement compositions are prepared by blending a CSA clinker comprising 54.3% ye'elimite and 29.1% belite with anhydrite and calcium oxide, respectively within the range [80–95%], [5-20%] and [0–15%]. Cement suspensions ($w/c = 6$) are maintained under stirring at 20°C for one month. The cement comprising 80% clinker and 20% anhydrite leads to the highest contents of ettringite and bound water, which is well simulated by thermodynamic calculations. Then, a kinetic study is performed on cement pastes ($w/c = 0.5$ or 0.6), the cement comprising 80% clinker and 20% CaSO_4 (introduced as anhydrite or gypsum). Gypsum, which dissolves faster than anhydrite, leads to the rapid formation of a dense microstructure, which tends to limit the progress of hydration at later age. With anhydrite, higher hydration degrees are reached and specimens cured in a wet or dry environment exhibit smaller volume changes.

1. Introduction

Self-desiccation of cement-based materials refers to their pore drying due to water consumption by hydration reactions (Powers, 1947; Jensen *et al.*, 2001; Chen *et al.*, 2013). A part of the mixing water is indeed chemically bound in the cement hydrates. A fine pore network is also created, which is capable of binding water physically by capillary condensation and surface adsorption. Self-desiccation is enhanced by a low water-to-cement ratio (w/c), a high chemical water demand of the cement (minimum amount of water required for full hydration of the cement anhydrous phases based on the stoichiometry of cement hydration), and sealed curing conditions (Li *et al.*, 2014). It is a desirable property for various applications. For instance, frost resistance is improved since an air-filled volume is created due to the chemical shrinkage (Persson, 2000). A low internal relative humidity close to the reinforcement bars may decrease their rate of corrosion (Persson, 1997). Besides, when the concrete needs to be covered by an impervious moisture-sensitive flooring, a fast decrease of the internal relative humidity of the concrete makes it possible to shorten the time until the covering can be applied (Andeberg, 2007). In the field of waste management, dry internal environments caused by self-desiccation are beneficial to mitigate the production of dihydrogen resulting from the corrosion of reactive metals such as aluminum (Hayes *et al.*, 2007; Zhou *et al.* 2006; McCague *et al.* 2017). A last example concerns the development of composite cement-based materials incorporating an oxide getter for the conditioning of tritiated waste (Lambertin *et al.*, 2010). The lowering of the internal relative humidity of the cement matrix notably improves the efficiency of the getter to trap H₂, HT or T₂.

Calcium sulfoaluminate cements (CSACs) with a high ye'elinite content are of interest to produce self-desiccating binders. Their hydration is usually fast and their chemical water demand, which depends on the hydrates assemblage, can be tailored by adjusting the composition of the cement. In the sulfoaluminate belite clinkers considered in this study,

ye'elimite predominates over belite, the second main anhydrous phase (Odler, 2000). Depending on the composition of the raw meal, the clinkers may also contain other minor phases such as calcium aluminates (CA, C₁₂A₇), gehlenite, excess anhydrite or calcium oxide (Sahu *et al.*, 1993). When the raw meal contains iron oxide, it may enter into the structure of ye'elimite, giving the solid solution C₄A_(3-x)F_xS, with x around 0.15 (Sharp *et al.* 1999; Chen *et al.* 1993). In addition, the ferrite phase (C₂(A, F)) may be formed, leading to ferroaluminate clinkers. CSACs are produced by intergrinding the clinkers with calcium sulfate (anhydrite, hemihydrate or gypsum), which is usually added in much higher amount (up to 15-25 weight % gypsum) than for Portland cement (a few weight %). Hydration of CSACs starts by the initial precipitation of ettringite and aluminum hydroxide (Eq. 1)¹, followed by the precipitation of calcium monosulfoaluminate hydrate and aluminum hydroxide (Eq. 2) once calcium sulfate is deficient (Zhang *et al.*, 2002; Winnefeld *et al.*, 2010, Torr ns-Martin *et al.*, 2013; Alvarez-Pinazo *et al.*, 2014).



Belite has a slower rate of hydration (Kasselouri *et al.*, 1995) and mainly yields str tlingite as long as AH₃ is present (Winnefeld *et al.*, 2010; Berger *et al.*, 2011) (Eq. 3).



Other silicate hydrates may also be encountered, such as siliceous hydrogarnet (Berger *et al.*, 2011) or C-S-H (Zhang *et al.*, 2002; Glasser *et al.*, 2001) which is formed in the absence or with very low contents of AH₃.

The contents of ettringite and calcium monosulfoaluminate hydrate are very sensitive to the amount of added calcium sulfate: ettringite dominates in a sulfate-rich environment, whereas the amount of calcium monosulfoaluminate hydrate tends to increase in a sulfate-deficient

¹ Shorthand cement notations are used : C = CaO, S = SiO₂, A = Al₂O₃, F = Fe₂O₃, \bar{S} = SO₃, T = TiO₂, M = MgO, H = H₂O

system. The initial calcium sulfate content not only influences the distribution of the hydrated products, but also the rate of hydration and the properties of the hardened CSAC-based materials. High calcium sulfate contents exert an accelerating effect on the rate of hydration at early ages (Berger *et al.*, 2011; Palou *et al.*, 1996). If properly formulated, rapid-hardening materials can be designed with limited shrinkage or even self-stressing properties (Pera *et al.*, 2004; Sherman *et al.*, 1995). On the contrary, low calcium sulfate contents tend to promote the development of very high mechanical strength at later ages (Berger *et al.*, 2011; Peysson, 2005; Winnefeld *et al.*, 2009). Besides, the chemical water demand of CSAC increases with the initial calcium sulfate content, up to a maximum which corresponds to the maximum precipitation of ettringite (the most water-rich hydrate). For instance, Glasser *et al.* (1998) calculated that, for a clinker containing 54.8 % ye'elimite and 27.4 % belite, the w/c ratio allowing complete hydration increased from 0.36 (0% gypsum) to 0.61 (30% gypsum). For comparison, the chemical water demand of a Portland cement corresponds to a w/c ratio close to 0.25 (Taylor, 1997). Dry internal environments are rather easily obtained in materials with a low water content. For instance, the internal relative humidity of two mortars prepared with w/c ratios of 0.38 and 0.3 reached 80% and 55% after a few months of hydration in closed environment (Glasser *et al.*, 2001).

The calcium sulfate content is not the sole factor to consider: its dissolution rate also plays a key role. Several authors compared the properties of CSACs prepared with gypsum or anhydrite. With gypsum, which dissolves faster than anhydrite, the CSAC exhibits a higher hydration degree after one day (Winnefeld *et al.*, 2010; Winnefeld *et al.*, 2010b; Allevi *et al.*, 2016; Majling *et al.*, 1985; Winnefeld *et al.*, 2017). Its setting and hardening are accelerated. However, at later ages, it may show a smaller mechanical strength than with anhydrite (Winnefeld *et al.*, 2009; Garcia Mate *et al.*, 2015; Pera *et al.*, 2003). Note however that Alvarez-Pinazo *et al.* (2016) report opposite results.

This literature review shows that, to design non-expansive materials leading to dry internal environments, the CSA cement composition should be taken into account, but also its rate of hydration which depends on the calcium sulfate source, as well as on the w/c ratio. This work thus investigates the influence of these three parameters on the amount of bound water in CSAC pastes or suspensions cured at ambient temperature. The study is performed in two stages. Experiments on suspensions (which make it possible to reach high degrees of hydration within a rather short period of time), associated with thermodynamic simulations, are first carried out to select a cement composition with a high chemical water demand. Then, the hydration of this cement is investigated in paste where several processes may limit the progress of hydration (e.g. lack of water, lack of space, difficult access to anhydrous phases). The influence of the calcium sulfate source and on the w/c ratio on the fraction of water actually bound by the cement pastes is thus determined.

2. Experimental

2.1 Raw materials

CSACs were prepared by mixing a ground industrial clinker (Vicat Alpenat^{UP}, $d_{10} = 3.3 \mu\text{m}$, $d_{50} = 12.0 \mu\text{m}$, $d_{90} = 42.4 \mu\text{m}$, Blaine surface area = $4650 \pm 150 \text{ cm}^2/\text{g}$) with analytical grade gypsum ($d_{10} = 3.2 \mu\text{m}$, $d_{50} = 14.3 \mu\text{m}$, $d_{90} = 43.9 \mu\text{m}$, specific surface area $\sim 0.5 \text{ m}^2/\text{g}$ measured by adsorption of N_2 using BET isotherm) or anhydrite ($d_{10} = 4.8 \mu\text{m}$, $d_{50} = 18.9 \mu\text{m}$, $d_{90} = 70.6 \mu\text{m}$, specific surface area $\sim 0.5 \text{ m}^2/\text{g}$) for 30 min using a Turbula mixer. The composition of the CSA clinker is reported in Table 1. The two main reactive phases were ye'elimite ($\text{C}_4\text{A}_3\bar{\text{S}}$) and belite (with the two polymorphisms $\alpha_{\text{H}}\text{'-C}_2\text{S}$ and $\beta\text{-C}_2\text{S}$). Merwinite (C_3MS_2), perovskite and maghemite ($\gamma\text{-Fe}_2\text{O}_3$) could be regarded as hydraulically inactive. Calcium oxide was produced by heating overnight analytical grade calcium hydroxide at 900°C . The dissolution rates of gypsum and anhydrite in water were compared by adding

known amounts of these two minerals into 250 mL demineralized water under magnetic stirring (100 r.p.m). The cell was thermostated at 25°C by circulating cooling water in a double envelope. The electrical conductivity was measured with a conductivity probe previously calibrated using a 12.88 mS/cm standardized KCl solution at 25°C.

2.2 Cement suspensions

2.2.1 Preparation

Ten cement compositions were investigated using design of experiments by blending CSA clinker with anhydrite (CaSO₄) and calcium oxide (CaO). The addition of CaO was expected to enhance the precipitation of ettringite according to reaction (Eq. 4), and thus to increase the chemical water demand of the binder.



The 3 investigated factors were thus the weight fractions of CSA clinker (X_1), anhydrite (X_2) and calcium oxide (X_3) in the blend. They checked equation (Eq. 5) which was characteristic of a three-component mixture problem.

$$x_1 + x_2 + x_3 = 1 \quad \text{with } x_i \text{ the level of factor } X_i \quad (\text{Eq. 5})$$

The factors were constrained between a lower limit a_i and an upper limit b_i ($0 \leq a_i < x_i < b_i < 1$), which were selected by taking into account data from the literature and results of some exploratory trials performed with extreme compositions.

- The domain of variation of the anhydrite fraction resulted from a compromise: too low contents (less than 5%) were avoided because they enhanced the formation of calcium monosulfoaluminate hydrate instead of ettringite. In the same way, too high contents (more than 20%) yielded self-stressing materials and were discarded. In the cements which did not contain any calcium oxide, the $C\bar{S}/C_4A_3\bar{S}$ molar ratio (referred as the M-value according to the Chinese classification of CSACs (Zhang *et al.*, 1994; Zhang *et*

al., 1999) varied from 0.43 to 2.1, which should correspond to binders with rapid setting and hardening properties ($0 < M < 1.5$) or to shrinkage compensated or slightly expansive materials ($1.5 < M < 2.5$).

- The minimal fraction of calcium oxide was set to 0%, which made it possible to investigate classical CSACs comprising CSA clinker and calcium sulfate. The maximum fraction of calcium oxide was limited to 15%. Winnefeld *et al.* (2009) have shown indeed that the addition of calcium hydroxide to CSAC strongly accelerates the precipitation of ettringite, but also leads to the initial precipitation of a calcium aluminate hydrate (C_4AH_n , $n = 13$ or 19) which causes a rapid loss of workability of the material in its fresh state, and can even produce false setting.
- As a consequence, the fraction of CSA clinker was comprised between 80% and 95%.

The resulting region of interest was a simplex (Figure 1). Response surface methodology is based on the hypothesis that the response (here the ratio between the weight of bound water and the initial weight of cement) can be approximated, within the range of the data, by a low-order polynomial model. The postulated model was a special cubic model in the canonical form (Eq. 6).

$$\eta = \beta_1 x_1 + \beta_2 x_2 + \beta_3 x_3 + \beta_{12} x_1 x_2 + \beta_{13} x_1 x_3 + \beta_{23} x_2 x_3 + \beta_{123} x_1 x_2 x_3 \quad (\text{Eq. 6})$$

with η the investigated response and β_i the model parameters to be estimated.

The positioning of the experimental points within the experimental domain is of great importance to obtain a good precision on the estimates of the model parameters and on the model-predicted response values. The 7 parameters of the model defined by (Eq. 6) were assessed using a simplex-lattice design introduced by Scheffé (1958). It included the 3 vertices of the simplex, the 4 edge centroids and the overall centroid. Three validation points corresponding to mixtures regularly distributed in the investigated domain and as remote as possible from the other selected points were added, for a total of 10 experiments. The

experimental data are summarized in Table 2. Three replicates of the overall centroid provided a measure of the experimental error.

The cement suspensions were prepared by adding 5 g of cement comprising CSA clinker, anhydrite and calcium oxide (proportions given in Table 2) to 30 g of deionized and decarbonated water (the water was previously boiled for one hour and cooled under nitrogen atmosphere). The polyethylene tubes containing the cement suspensions were tightly closed under nitrogen atmosphere and stirred for one month at ambient temperature ($22 \pm 2^\circ\text{C}$) using a rotary shaker.

2.2.2 Characterization

After one month, the suspensions were filtrated under vacuum at $0.45 \mu\text{m}$. The solid fractions were rinsed with isopropanol and dried for 7 days in a controlled humidity chamber (with a 23% relative humidity at $22 \pm 2^\circ\text{C}$ controlled by a saturated solution of potassium acetate). Berger (2009) has shown that, under these conditions, a strong dehydration of ettringite (resulting in a decrease or loss of its diffraction peaks by XRD) is avoided. The powders were then characterized using thermogravimetry and X-ray diffraction.

Thermogravimetric analyses (TGA) were carried out using a TGA/DSC Netzsch STA 409 PC instrument. The samples were heated under nitrogen (gas flow set at 50 mL/min) at $10^\circ\text{C}/\text{min}$ up to 800°C . The curves were corrected from buoyancy effects by performing a blank subtraction. The ratio between the mass of bound water and the initial mass of cement (bw/c) was calculated using equation (Eq. 7).

$$\text{bw/c} = (m_{25^\circ\text{C}} - m_{600^\circ\text{C}}) / m_{800^\circ\text{C}} \quad (\text{Eq. 7})$$

with $m_{25^\circ\text{C}}$, $m_{600^\circ\text{C}}$ and $m_{800^\circ\text{C}}$ the weights of the samples at 25°C , 600°C and 800°C given by the thermograms. Some samples exhibited a small weight loss at 680°C corresponding to the decarbonation of calcite. This weight loss was thus not taken into account for the calculation

of the mass of bound water. Note that the bound water determined using this technique corresponded to water chemically bound in the cement hydrates, but also likely to water strongly adsorbed on the cement particles.

Crystallized phases were qualitatively analysed by powder X-ray diffraction using the Debye-Scherrer configuration (transmission mode) (PanAlytical X'pert Pro, copper anode, $\lambda_{K\alpha 1}=1.5418 \text{ \AA}$, scanning from $2\theta = 5^\circ$ to 120° in 0.017° steps, for a total counting time of 6 h). The samples were introduced in Lindeman tubes ($\Phi = 0.7 \text{ mm}$) and mounted on a spinning goniometric head during measurement to reduce the preferred orientation effect. Powders were finely ground by hand at a particle size below $100 \text{ }\mu\text{m}$ with silicon used as an internal standard.

2.2.3 Thermodynamic modeling

The experiments were supported by thermodynamic equilibrium modeling in order to predict the mineralogy of the fully hydrated cements. The thermodynamic calculations were carried out using GEMS software (Kulik *et al.*, 2013) which works by minimizing the Gibbs free energy of a pre-defined system and computes its phase assemblage and speciation at equilibrium knowing its total bulk elemental composition. The thermodynamic data for aqueous species and cement phases were taken from the PSI-GEMS (Thoenen *et al.*, 2014) and cement-specific CEMDATA 14.01 (Matschei *et al.*, 2007; Lothenbach *et al.*, 2012) thermodynamic databases. Hydration was simulated for the 28 compositions of CSAC reported in Table 2. For the calculations, some phases of the clinker were neglected due to their low reactivity (C_3MS_2 , $\gamma\text{-Fe}_2\text{O}_3$, C_3FT) or low content (C_6AF_2).

2.3 Cement pastes

2.3.1 Preparation

The cement comprised 80 wt.% clinker and 20 wt.% calcium sulfate, introduced either as anhydrite or as gypsum. Its M value ($C\bar{S}/C_4A_3\bar{S}$ ratio) was 2.1. Pastes were prepared with w/c ratios of 0.5 and 0.6. These ratios, which are typical of fluid grouts, were smaller than the chemical water demand of the cement (corresponding to a w/c ratio of 0.62 – see section 3.1.2), which means that a fraction of the cement should remain unhydrated. When gypsum was used as the calcium sulfate source, the water brought by this mineral was taken into account to calculate the w/c ratio. Cement and water (in the proportions given in Table 3) were mixed for 5 min using a standardized laboratory mixer (following European standard EN 196-1) rotating at low speed. Paste samples were cast into airtight polypropylene boxes (20 mL of paste per box) and cured at $25 \pm 1^\circ\text{C}$ for a period of time ranging from 1 d to 90 d, before being characterized to determine their mineralogy and microstructure (section 3.2.2). Three moulds of 4x4x16 cm specimens equipped with measurement gauges were also prepared and cured for 24 h in a climatic chamber at 20°C and 95% R.H. The specimens were then demoulded, weighed, measured, and submitted to different curing conditions: in sealed bag or under water at room temperature ($22 \pm 2^\circ\text{C}$) or at 38°C and 100% H.R. in a climatic chamber.

2.3.2 Characterization

Hydration of the cement pastes was investigated using a TAM AIR conduction microcalorimeter under isothermal conditions at 25°C . Calorific capacities of solution and cement were respectively taken equal to 3.76 and 0.75 J/ $^\circ\text{C}$ /g. Mixing of the dry cement and solution was performed outside the calorimeter. About 2 g of cement paste was cast in a glass ampoule and introduced in the calorimeter. The heat flow was recorded versus time and compared to that of a sample maintained at 25°C and consisting of water, the volume of which being adjusted to get the same calorific capacity as the paste sample.

Cement hydration was stopped after fixed periods of time by successively immersing the crushed paste into isopropanol, filtrating the suspension and drying it for 7 days in a controlled humidity chamber at 22 ± 2 °C and 23% relative humidity. The powders were then characterized by thermogravimetry and X-ray diffraction using the procedures described in section 2.2.2.

After demoulding (1 d after the mixing), the 4x4x16 cm specimens were weighed, measured, and submitted to different curing conditions: in sealed bag and under water at room temperature (22 ± 2 °C) or at 38°C and 100% H.R. in a climatic chamber. Their length and mass changes were measured after curing periods of 7 d, 28 d, 60 d and 90 d. The specimens cured at 38°C were cooled in a climatic chamber at 20°C and 95% R.H. for 4 hours before their characterization.

3. Results and discussion

3.1 Cement suspensions

3.1.1 Phase assemblage of the solid fractions

Hydration of CSAC in paste is a long process which lasts for several months. To reach an advanced hydration degree within a reasonable period of time and assess the amount of bound water, the experiments were first carried out in suspension (w/c ratio of 6). Berger *et al.* (2011) have shown indeed that a CSAC (clinker with 68.5% $C_4A_3\bar{S}$, 15.9% C_2S and 9.5% $C_{12}A_7$) containing 20% gypsum is fully hydrated after 7 days of stirring at 25°C with water in excess (w/c ratio of 10).

Figure 2 shows the diffraction patterns of the solid fractions collected from the suspensions after one month of stirring. The phase assemblage depended on the initial composition of the cement. The binders with a high content of anhydrite and a low content of CaO (trials #2, #4 and #9) mainly produced ettringite, with traces of monosulfate. Reversely, the cements with a

low content of anhydrite and a high contents of CaO (trials #3, #5, #10) mainly yielded monosulfate, ettringite being either absent or present as traces. The two cements with the highest CaO content did not produce (# 3) or produced (#10) only traces of strätlingite. Katoite was present in all samples, excepting the solid fraction of sample #2 (80% clinker, 20% CaSO₄). Belite was clearly evidenced in sample #3 (80% clinker, 5% CaSO₄, 15% CaO), meaning that hydration of the cement was not complete after one month in this sample. The possible presence of residual belite in the other samples could not be ruled out: this phase would be responsible for the left shoulder of the diffraction peak of ettringite recorded at $2\theta = 31.9^\circ$.

The solid fractions of the suspensions were also characterized by TGA. Figure 3 shows the derivative weight loss of the different samples as a function of temperature (Table 4). The assignment of the different peaks was complex because the dehydration temperature ranges of the hydrates possibly present in the samples overlapped. In particular, C-S-H could not be clearly evidenced since it exhibits its main weight loss between 100 and 150°C, a temperature range in which ettringite, monosulfate and strätlingite also dehydrate. Nevertheless, the results confirmed the massive precipitation of:

- ettringite in suspensions #2, #4 and #9 prepared with CaSO₄-rich cements,
- monosulfate in suspensions #3 and #10 prepared with CaO-rich cements,

The samples could also contain poorly crystallized aluminum hydroxide which would be responsible for the weight loss close to 260°C. In sample #3, the weight loss around 310°C might be explained by the dehydration of katoite, a mineral also evidenced by X-ray diffraction.

The phases precipitated at thermodynamic equilibrium in 28 suspensions located within the composition domain of interest were calculated using GEMS software and the CEMDATA database. Five phase assemblages were obtained (Figure 4):

- monosulfate + ettringite + gibbsite + strätlingite for clinker / anhydrite binary blends with a fraction of anhydrite $\leq 17.5\%$,
- ettringite + gibbsite + strätlingite + C-S-H for the cement comprising 20% anhydrite and 80% clinker,
- monosulfate + ettringite + strätlingite + C-S-H for ternary blends with low or intermediate contents of CaO,
- monosulfate + strätlingite + C-S-H or monosulfate + strätlingite + C-S-H + C_3AH_6 for ternary blends with high contents of CaO.

Monosulfate and C-SH showed variable compositions within the domain of interest:

- the Ca/Si ratio of C-S-H increased from 0.86 (in the absence of CaO) to 1.6 (when the CaO fraction was at its maximum),
- monosulfate was in fact a solid solution between $C_3A.C\bar{S}.H_{12}$ and C_4AH_{13} , noted $x C_3A.C\bar{S}.H_{12} \cdot (1-x) C_4AH_{13}$ with x varying from 0.99 (in the absence of CaO) to 0.80 (when the CaO fraction was at its maximum).

As expected, increasing the anhydrite content promoted the formation of ettringite against that of monosulfate in a binary blend comprising initially clinker and anhydrite. In a ternary blend, when the fraction of clinker or anhydrite was maintained constant, increasing the fraction of CaO (and thus decreasing the fraction of the third component) tended to increase the amount of monosulfate precipitated, and to decrease those of ettringite and strätlingite. Given the relatively high content of belite compared to ye'elimeite in the clinker, there was thus no interest in adding supplementary calcium oxide to enhance the amount of ettringite formed by hydration.

The calculated phase assemblages were compared to the experimental ones for suspensions #1 to #10. The two series of results showed similarities.

- According to the calculations, ettringite did not precipitate in suspensions #3, #5 and #10; experimentally, it was absent (#3) or present as traces (#5, #10).
- Monosulfate did not precipitate in suspension #2 according to the simulation and the experiment.
- Katoite (C_3AH_6), which was predicted to form in suspension #3, was actually evidenced by XRD. Note that the diffraction peaks were slightly shifted as compared with the JCPDS file reference, which may in fact suggest the presence of a solid solution between C_3AH_6 and C_3AS_3 (Jappy *et al.*, 1992) (not included in the thermodynamic model).

However, some differences were also noticed:

- according to the simulations, all the samples should contain strätlingite, but this mineral was not observed in suspension #3,
- the presence of gibbsite was predicted only in suspensions #1, #2 and #4, but experimentally, it seemed likely in all the samples.

These differences could be explained by an uncomplete hydration of cement. The residual presence of belite in the experimental suspensions was suspected from the XRD data. This phase, which hydrates more slowly than ye'elimite, yields strätlingite in the presence of AH_3 (Eq. 3), and C-S-H when AH_3 is deficient. A partial reaction of belite should thus influence the contents of these 3 hydrates.

3.1.2 Bound water

The water demand of the investigated cements, expressed as the ratio between the bound water and the initial mass of cement (bw/c), was calculated according to equation (Eq. 7)

using the TGA results (Table 5). The binary blend comprising 80% clinker and 20% anhydrite (#2), which formed the highest amount of ettringite, also had the highest water demand ($bw/c = 0.61$).

The variations of the bw/c ratio were fitted using a special cubic model in the canonical form (Eq. 6) as a function of the initial cement composition (fractions of clinker, anhydrite and calcium oxide). The models coefficients were estimated using standard least squares regression techniques (Table 6). Possible model deficiencies were looked for by using analysis of variance (ANOVA). The model provided a good correlation of the experimental data and was regarded as an acceptable prediction tool. The bw/c ratio was at its maximum for the cement with the highest content of anhydrite located at one vertex of the simplex (#2), which formed the highest amount of ettringite (Figure 5). Reversely, the ternary blend comprising 80% clinker, 5% anhydrite and 15% calcium oxide (#3), which did not produce ettringite, led to the smallest bw/c ratio (0.35).

The chemical water demand of the different cements was also calculated by thermodynamic modeling. The results were in rather good agreement with the experimental ones, except for cement #3 (Table 5, Figure 5). In that case, the experimental bw/c ratio was notably below the calculated ratio, which resulted from the fact that the cement hydration in suspension #3 was not at its end (belite was evidenced by XRD in the solid fraction of suspension #3 after one month of stirring). Note finally that the experimental bw/c ratios of suspensions #1, #4, #7, #8 and #9 slightly exceeded the simulated ratios. Two hypotheses may explain this small difference.

- In the simulation, the hydration of ferrite was neglected. Taking it into account would slightly increase the calculated chemical water demand.
- In the experiments, the samples were submitted to “soft” drying to limit the dehydration of ettringite. The presence of sorbed water, in addition to water bound in

the structure of the hydrates, is likely, which leads to overestimate the chemical water demand.

3.2 Cement pastes

The cement containing 80% clinker and 20% calcium sulfate, which led to the highest bw/c ratio in suspension, was selected for further investigation in paste.

3.2.1 Dissolution rates of gypsum and anhydrite

Figure 6 compares the evolution of the electrical conductivity of demineralized water with increasing amounts of gypsum or anhydrite (from 7.6 mmol/L to 1200 mmol/L). The conductivity increased due to the release of Ca^{2+} and SO_4^{2-} ions in solution and levelled off when the minerals were fully dissolved (experiments at 7.6 mmol/L), or when the solubility limit of gypsum was reached (14.9 to 15.7 mmol/L at 25°C (Hardie, 1967)). Whatever the investigated concentration, the time needed to reach the conductivity plateau was much shorter for gypsum than for anhydrite, indicating a faster dissolution rate.

3.2.2 Hydration rate of cement pastes

Hydration of the cement pastes was monitored by isothermal conduction calorimetry. The first minutes were characterized by heat generation which resulted from several factors: start of dissolution of ye'elite, but also, and mainly, introduction of the externally prepared sample in the calorimetric chamber, which biased the signal. The heat flow produced by the different cement pastes was thus recorded from 30 minutes onwards (Figure 7). The period of low thermal activity was short: it lasted ~ 0.6 h with gypsum, and 0.8 to 0.9 h with anhydrite. The w/c ratio had little influence on the hydration rate. With gypsum, the heat flow showed one main peak (maximum at 1.6 h, with possibly one shoulder), followed by a second one of

smaller magnitude (maximum at 7 h). According to Winnefeld *et al.* (2010), the main peak is due to the massive consumption of ye'elimite to form ettringite and AH_3 (Eq. 1), and the second one is caused by the depletion of sulfate and calcium ions from the solution, leading to the precipitation of monosulfate and AH_3 (Eq. 2). The area of the first peak was smaller with anhydrite. Dissolution of anhydrite being slower than that of gypsum, this may result in an undersupply of calcium and sulfates which would limit the period of massive dissolution of ye'elimite to form ettringite. Several authors noticed that the amount of ettringite precipitated at early ages is smaller if the cement contains anhydrite rather than gypsum (Sahu *et al.*, 1991; Pera *et al.*, 2003). The cumulative heats are compared in Figure 7. The pastes with anhydrite had a higher heat of hydration (82 J/g of clinker at $w/c = 0.5$, 86 J/g at $w/c = 0.6$) than those with gypsum. This difference could not be only explained by the fact that the dissolution of anhydrite is exothermic ($\Delta H = -21 \text{ kJ}\cdot\text{mol}^{-1}$) whereas that of gypsum is slightly endothermic ($\Delta H = 0.75 \text{ kJ}\cdot\text{mol}^{-1}$) (Perry, 1984): in such a case, the heat difference should be of 40 J/g for the pastes under investigation (containing 1.84 mmol of gypsum or anhydrite for 1 g of clinker). The additional heat produced with anhydrite was likely due to a more advanced dissolution of the cement anhydrous phases. Increasing the w/c ratio from 0.5 to 0.6 also increased the cumulative heat, regardless of the calcium sulfate source, which indicated that higher hydration degrees were reached with a higher water content.

3.2.3 Mineralogical evolution

The cement pastes were characterized by X-ray diffraction (Figure 8, Figure 9). The highest degree of hydration seemed to be obtained with paste AN-06 (with anhydrite and a w/c ratio of 0.6):

- ye'elimite was not detected anymore from the first characterization time,
- small amounts of monosulfate were observed from 23 d onwards,

- at 90 d, belite had reacted to form significant amounts of strätlingite.

When the w/c ratio was decreased to 0.5, the 90 d-old sample contained only small amounts of strätlingite, and traces of monosulfate.

With gypsum, regardless of the w/c ratio, exhaustion of ye'elimite was not observed over the duration of the study, nor the precipitation of any crystallized silicate hydrate. Ettringite was the main hydrate formed, with possible traces of monosulfate at 90 d.

The thermograms of the pastes (Figure 10) showed that they also contained aluminum hydroxide (responsible for the weight loss at 260°C). Its depletion to form strätlingite according to reaction (Eq. 3) after 24 h was well evidenced in paste AN-06 (with anhydrite and a w/c ratio of 0.6).

3.2.4 Bound water in the cement pastes

The amount of bound water in the cement pastes was assessed from their weight loss at 600°C (measured by TGA). Table 7 compares the bw/c ratio of the different paste samples (where c stands for the initial mass of cement, i.e. the mass of clinker + CaSO₄). For a given hydration time, the bw/c ratio increased with the w/c ratio of the cement paste. This result confirmed the calorimetric data which showed higher heats of hydration, and thus higher hydration degrees, when the w/c ratio was set to 0.6 instead of 0.5. When the calcium sulfate was brought as gypsum, the amount of bound water exhibited almost no change between 1 and 23 d. In contrast, when the clinker was blended with anhydrite, the amount of bound water went on increasing from 1 to 7 d. The highest bw/c ratio (0.48) was obtained for paste AN-06 (with anhydrite). Polished sections of the 1 d-old cement pastes were observed using scanning electron microscopy (Figure 11). Different microstructures were observed. Paste AN-06 contained many microporous zones with large ettringite crystals, together with denser regions mainly comprising aluminum hydroxide. In paste GY06, ettringite and aluminum hydroxide

were more homogeneously distributed within the matrix which seemed to be less porous. Allevi *et al.* (2016) also noted a difference of crystal morphology for ettringite precipitated in pastes prepared with anhydrite or gypsum: with anhydrite, needle-like crystals of ettringite formed while, with gypsum, smaller crystals were obtained, forming a denser microstructure. This denser microstructure at early age might possibly contribute to slow down the subsequent progress of hydration because of a more difficult access to the anhydrous phases or water, or a lack of space for the precipitation of hydrates.

Table 8 summarizes the amounts of free water and bound water in 1 L of the different cement pastes at 90 d. Hydration of cement was less advanced in paste AN-05 (with anhydrite and a w/c ratio of 0.5) than in paste AN-06, but since paste AN-05 contained less total water than paste AN-06, its amount of free water was finally smaller.

3.2.5 *Volume stability of hardened cement pastes*

The length change and mass gain of the hardened paste specimens were studied under different curing conditions:

- in sealed bag at room temperature, to investigate the evolution of the materials with no (or limited) interaction with the environment,
- under water at room temperature, or at 38°C and 100% R.H. (conditions commonly used in the field of nuclear waste management to check the stability of cemented wasteforms) to promote the development of expansive processes. The results are summarized in Figure 12.

As expected, the bars cured in wet environment (under water at room temperature, or at 38°C and 100% R.H.) exhibited swelling and mass increase. This latter could result from several processes: water uptake due to capillary suction to compensate for water depleted by hydration, water penetration due to osmosis (the interstitial solution being more

concentrated than the curing solution), and continuation of hydration. The swelling, which did not induce any cracks over the 3 months of the study, was much stronger with gypsum than with anhydrite. Similar results have already been reported by Chen *et al.* (2012). Several hypotheses may be postulated to explain this result.

- The samples with gypsum contained higher amounts of residual ye'elimite when they were placed under wet conditions. The restart of hydration may thus be more important, leading to mineralogical evolutions with possible volume increase, such as retarded ettringite formation and precipitation of strätlingite from C_2S and AH_3 ($\Delta V/V = + 3.5\%$).
- Several authors have shown that, because of its reactivity higher than that of anhydrite, gypsum leads to higher supersaturation of the pore solution with respect to the sulfate-rich hydrates (ettringite, monosulfoaluminate), which increases their crystallization pressure (Chaunsali *et al.*, 2015; Bizzozero *et al.*, 2014).

Decreasing the w/c ratio of the pastes from 0.6 to 0.5 seemed to increase slightly their swelling. This again could result from the restart of hydration. When the specimens were placed under curing, cement hydration was less advanced in the pastes at w/c = 0.5 than in those at w/c = 0.6. Differences in microstructures might also be involved, such as a smaller pore volume available for the precipitation of hydrates in the samples at w/c = 0.5 or a finer pore network.

The length change of the specimens cured in sealed bag depended on two antagonistic processes:

- creation of empty porosity due to water depletion by cement hydration and desiccation (the samples exhibited a small weight loss (0.4 to 0.6%) after 90 d). The water / air menisci created in the partly empty pores induced shrinkage, the magnitude of which

depended on the diameter of the pores being emptied: the lower the pore diameter, the lower the stress;

- expansion due to the crystallization of hydrates.

The shrinkage was more important with gypsum than with anhydrite, and was almost compensated for paste AN-06 with the highest degree of hydration. In all cases, it did not vary significantly after 28 d.

Using anhydrite instead of gypsum could thus be recommended to improve the volume stability of the hardened CSAC pastes whatever the curing conditions.

4. Conclusion

This work investigated the influence of the CSAC composition and calcium sulfate source on the content of water bound by hydration when the cement was hydrated in suspension ($w/c = 6$) or in paste ($w/c = 0.5$ or 0.6). It led to the following conclusions.

1. The chemical water demand of a CSA cement strongly depends on its composition. It varies within the range 0.44-0.62 for ternary blends comprising clinker (54.3 wt.% ye'elimite, 29.1 wt.% belite) [80 – 95%], calcium sulfate [5 - 20%] and calcium oxide [0 – 15%], which is well simulated by thermodynamic modelling. The maximum is obtained for the cement comprising 80% clinker and 20% CaSO_4 leading to the maximum amount of ettringite. Increasing the calcium content of the cement by an addition of calcium oxide has a depressive effect on the chemical water demand.

2. For a given composition of cement, the dissolution rate of calcium sulfate has a strong influence on the amount of water actually bound by the cement paste. Anhydrite, which dissolves more slowly than gypsum, makes it possible to reach higher degrees of hydration. For pastes prepared with a cement comprising 80% clinker and 20% CaSO_4 , (introduced as anhydrite or gypsum) and a w/c of 0.6, the fraction of bound water at 90 d is close to 80%

with anhydrite, 70% only with gypsum. Gypsum leads to the massive precipitation of small crystals of ettringite during the first hours of hydration, forming a dense structure which might contribute to limit the subsequent progress of hydration.

3. Decreasing the w/c ratio also produces a denser microstructure of the paste, and tends to decrease the fraction of bound water at later age.

4. Using anhydrite instead of gypsum not only increases the fraction of water bound by cement hydration, but also significantly improves the volume stability of the hardened material when it is cured under wet environment or in sealed bag.

Future work will thus be focused on the design and characterization of mortar and concrete materials for different field applications using a CSA cement comprising 80% clinker and 20% anhydrite.

5. Acknowledgements

This work is supported by Andra as part of the program “Investissements d’Avenir” of the French government.

6. References

Allevisi S, Marchi M, Scotti F, Bertini S, Cosentino C (2016) Hydration of calcium sulfoaluminate clinker with additions of different calcium sulphate sources. *Mater. Struct.* **49**: 453-466.

Anderberg A (2007) *Studies of Moisture and Alkalinity in Self-Levelling Flooring Compounds*, PhD-thesis, Division of Building Materials, Faculty of Engineering Lund University, Lund.

- Álvarez-Pinazo G, Cuesta A, García-Maté M, Santacruz I, Losilla ER, Sanfélix SG, Fauth F, Aranda MAG, De la Torre AG (2014) In-situ early-age hydration study of sulfobelite cements by synchrotron powder diffraction. *Cem. Concr. Res.* **56**: 12-19.
- Álvarez Pinazo G, Santacruz I, Aranda MAG, de la Torre AG (2016) Hydration of belite-ye'elinite-ferrite cements with different calcium sulfate sources. *Adv. Cem. Res.* **28**: 453-466.
- Berger S (2009) *Etude des potentialités des ciments sulfo-alumineux bélitiques pour le conditionnement du zinc. De l'hydratation à la durabilité.* PhD thesis, University of Lille 1, France, 248 p.
- Berger S, Cau Dit Coumes C, Le Bescop P, Damidot D (2011) Influence of a thermal cycle at early age on the hydration of calcium sulfoaluminate cements with variable gypsum contents. *Cem. Concr. Res.* **41**: 149-160.
- Bizzozero J, Gosselin C, Scrivener KL (2014) Expansion mechanisms in calcium aluminate and sulfoaluminate cements with calcium sulfate. *Cem. Concr. Res.* **56**: 190-202.
- Chaunsali P, Mondal P (2015) Influence of calcium sulfoaluminate (CSA) cement content on expansion and hydration behaviour of various Ordinary Portland cement-CSA blends. *J. Amer. Ceram. Soc.* **98**: 2617-2624.
- Chen D, Feng F, Long S (1993) The influence of ferric oxide on the properties of $3\text{CaO}\cdot 3\text{Al}_2\text{O}_3\cdot \text{CaSO}_4$. *Thermochimica Acta* **215**: 157-169.
- Chen IA, Hargis CW, Juenger MCG (2012) Understanding expansion in calcium sulfoaluminate-belite cements. *Cem. Concr. Res.* **42**: 51-60.
- Chen H, Wyrzykowski M, Scrivener K, Lura P (2013) Prediction of self-desiccation in low water-to-cement ratio pastes based on pore structure evolution. *Cem. Concr. Res.* **49**: 38-47.
- Fleischer M, Jambor J (1977) New mineral names. *Am. Mineral.* **62**: 395-397.

- Frontera C, Rodriguez-Carvajal J (2003) FullProf as a new tool for flipping ratio analysis. *Physica B* **335**: 219–222.
- Garcia Mate M, de la Torre AG, Leon-Reina I, Losilla ER, Aranda MAG, Santacruz I (2015) Effect of calcium sulfate source on the hydration of calcium sulfo-aluminate eco-cement. *Cem. Concr. Comp.* **55**: 53-61.
- Glasser FP, Zhang L (1998) Calculation of chemical water demand for hydration of calcium sulfoaluminate cement, *Proc. 4th International Symposium on Cement and Concrete, Shanghai, pp. 38-44.*
- Glasser FP, Zhang L (2001) High-performance cement matrices based on calcium sulfoaluminate-belite compositions. *Cem. Concr. Res.* **31**: 1881-1886.
- Hardie LA (1967) The gypsum-anhydrite equilibrium at one atmosphere pressure. *Am. Miner.* **52**: 171-200.
- Hayes M, Godfrey IH (2007) Development of the use of alternative cements for the treatment of intermediate level waste. *Proc. Waste Management 2007 (WM'07) Conference, Tucson, USA.*
- Jappy TG, Glasser FP (1992) Synthesis and stability of silica-substituted hydrogarnet $\text{Ca}_3\text{Al}_2\text{Si}_{3-x}\text{O}_{12-4x}(\text{OH})_{4x}$. *Adv. Cem. Res.* **4**: 1–8.
- Jensen OM, Hansen PF (2001) Autogenous deformation and RH-change in perspective. *Cem. Concr. Res.* **31**: 1859–65.
- Kasselouri V, Tsakiridis P, Malami C, Georgali B, Alexandridou C (1995) A study on the hydration products of a non-expansive sulfoaluminate cement. *Cem. Concr. Res.* **25** : 1726-1736.
- Kulik D, Wagner T, Dmytrieva SV, Kosakowski G, Hingerl F, Chudnenko KV, Berner U (2013) GEM-Selektor geochemical modeling package: revised algorithm and GEMS3K numerical kernel for coupled simulation codes. *Comput. Geochem.* **17**: 1–24.

- Lambertin D, Cau Dit Coumes C, Frizon F, Jousset-Dubien C (2010) *Matériau pour le Piégeage d'Hydrogène, Procédé de Préparation et Utilisations*. Patent WO/2010/066811.
- Li K, Zeng Q, Luo M., Pang X (2014) Effect of self-desiccation on the pore structure of paste and mortar incorporating 70% GGBS. *Constr. Build. Mater.* **51**: 329-337.
- Lothenbach B, Pelletier-Chaignat L, Winnefeld F (2012) Stability in the system CaO-Al₂O₃-H₂O. *Cem. Concr. Res.* **42**: 1621–1634.
- Majling J, Znasik R, Gabrisova A, Svetik S (1985) The influence of anhydrite activity upon the hydration of calcium sulfoaluminate cement clinker. *Thermochim. Acta* **92**: 349-352.
- Matschei T, Lothenbach B, Glasser FP (2007) Thermodynamic properties of Portland cement hydrates in the system CaO-Al₂O₃-SiO₂-CaSO₄-CaCO₃-H₂O. *Cem. Concr. Res.* **37**: 1379–1410.
- McCague C, Zhou J, Basheer M, Bai Y (2017) Low-pH cement composites for the encapsulation of nuclear wastes containing aluminium. *Proc. The Future of Cement 2017, Paris, France*.
- Odler I (2000) *Special Inorganic Cements*. Taylor and Francis ed., London, 395 p.
- Palou MT, Majling J (1996) Effects of sulphate, calcium and aluminum ions upon the hydration of sulphoaluminate belite cement. *J. Thermal Anal.* **46**: 549-556.
- Pera J, Ambroise J, Holard E, Beauvent G (2003) Influence of the type of calcium sulfate on the properties of calcium sulfoaluminate cement, *Proc. 11th International Congress on the Chemistry of Cements, Durban, South Africa May 11-16*, **3**: 1129-1135.
- Pera J, Ambroise J (2004) New applications of calcium sulfoaluminate cement. *Cem. Concr. Res.* **34**: 671-676.
- Perry JH (1984) *Chemical Engineering Handbook, Section 3*. 5th Edition, Mc Graw Hill, pp 157-159.

- Persson B (1997) Self-desiccation and its importance in concrete technology. *Mater. Struct.* **30**: 293–305.
- Persson B (2000) Consequence of cement constituents, mix composition and curing conditions for self-desiccation in concrete. *Mater Struct.* **33**: 352-362.
- Powers TC (1947) A discussion of cement hydration in relation to the curing of concrete. *Proc. Highw. Res. Board* **27**: 178–188.
- Peysson S (2005) *Contribution à l'étude de la stabilisation de déchets par du ciment sulfo-alumineux*. PhD Thesis, INSA Lyon, France.
- Pöllmann H (1984) Die Kristallchemie des Neubildungen bei Einwirkung von Schadstoffen auf hydraulische Bindemittel. Doktorgrades, Friedrich Alexander Universität Erlangen-Nürnberg.
- Rivas-Mercury JM, Pena P, de Aza AH, Turrillas X (2008) Dehydration of $\text{Ca}_3\text{Al}_2(\text{SiO}_4)_y(\text{OH})_{4(3-y)}$ ($0 < y < 0.176$) studied by neutron thermodiffractometry. *J. Eur. Ceram. Soc.* **28**: 1737–1748.
- Saika N, Kato S, Kojima T (2006) Thermogravimetric investigation on the chloride binding behavior of MK-lime paste, *Thermochim. Acta* **444**: 16-25.
- Sahu S, Havlica J, Tomkova V, Majling J (1991) Hydration behavior of sulphoaluminate belite cement in the presence of various calcium sulphates. *Thermochim. Acta* **175**: 45-52.
- Sahu S, Majling J (1993) Phase compatibility in the system $\text{CaO-SiO}_2\text{-Al}_2\text{O}_3\text{-Fe}_2\text{O}_3\text{-SO}_3$ referred to sulphoaluminate belite cement clinker. *Cem. Concr. Res.* **23**: 1331-1339.
- Sharp JH, Lawrence CD, Yang R (1999) Calcium Sulfoaluminate Cements – low-energy cements, special cements or what ?. *Adv. Cem. Res.* **11**: 3-13.
- Scheffé H (1958) Experiments with mixtures. *J. R. Stat. Soc. Ser. B.* **20** : 344-360.

- Sherman N, Beretka J, Santoro L, Valenti GL (1995) Long-term behavior of hydraulic binders based on calcium sulfoaluminate and calcium sulfosilicate. *Cem. Concr. Res.* **25** : 113-126.
- Taylor HFW (1997) *Cement chemistry*. 2nd Edition, Thomas Telford, London, pp197-199.
- Thoenen T, Hummel W, Berner U, Curti E (2014) *The PSI/Nagra Chemical Thermodynamic Database 12/07*. PSI report 14-04, Villigen PSI, Switzerland.
- Torréns-Martín D, Fernández-Carrasco L, Martínez-Ramírez S (2013) Hydration of calcium aluminates and calcium sulfoaluminate studied by Raman spectroscopy. *Cem. Concr. Res.* **47**: 43-50.
- Ukrainczyk N, Matusinovic T, Kurajica S, Zimmermann B, Sipusic J (2007) Dehydration of a layered double hydroxide – C₂AH₈. *Thermochim. Acta* **464**: 7-15.
- Wenda R (1984) *Untersuchungen zur Kristallchemie des Hydrationsprodukte borathaltiger Zemente*. Doktorgrades, Friedrich Alexander Universität Erlangen-Nürnberg.
- Winnefeld F, Barlag S (2009) Influence of calcium sulfate and calcium hydroxide on the hydration of calcium sulfoaluminate clinker. *Zement Kalk Gips* **6**: 42-53.
- Winnefeld F, Lothenbach B (2010) Hydration of calcium sulfoaluminate cements – Experimental findings and thermodynamic modelling. *Cem. Concr. Res.* **40**: 1239-1247.
- Winnefeld F, Barlag S (2010b) Calorimetric and thermogravimetric study on the influence of calcium sulfate on the hydration of ye'elimite. *J. Thermal Anal. Calorim.* **101**: 949-957.
- Winnefeld F, Martin LHJ, Müller CJ, Lothenbach B (2017) Using gypsum to control hydration kinetics of CSA cements. *Constr. Build. Mater.* **155**: 154-163.
- Zhang L, Su M, Wang Y (1994) The third cement series in China. *World Cem.* **25**: 6–10.
- Zhang L, Su M, Wang Y (1999) Development of the use of sulfo- and ferroaluminate cements in China. *Adv. Cem. Res.* **11**: 15–21.

Zhang L, Glasser FP (2002) Hydration of calcium sulfoaluminate cement at less than 24 hours. *Adv. Cem. Res.* **14**: 141-155.

Zhou Q, Milestone NB, Hayes M (2006) An alternative to Portland Cement for waste encapsulation - The calcium sulfoaluminate cement system. *J. Hazard. Mater.* **136**: 120-129.

Table 1: Oxide* and phase** composition of the CSA clinker (Vicat Alpenat^{UP})

Oxide	SiO ₂	Al ₂ O ₃	Fe ₂ O ₃	CaO	MgO	TiO ₂	Mn ₂ O ₃	P ₂ O ₅	SrO	Na ₂ O	K ₂ O	SO ₃	Cl ⁻	LOI
Wt %	10.55	23.46	9.70	45.07	1.00	1.29	0.01	0.11	0.06	0.17	0.27	8.07	0.01	0.23

Minerals	C ₄ A ₃ \bar{S} (solid solution)	β -C ₂ S	α' -C ₂ S	C ₃ MS ₂	CaO	γ -Fe ₂ O ₃	C ₃ FT	C ₆ AF ₂
Wt %	54.3 ± 1.4	20.8 ± 1.8	8.3 ± 0.8	4.5 ± 1.0	0.2 ± 0.1	1.0 ± 0.2	9.3 ± 0.4	1.2 ± 0.2

*: determined by X-ray fluorescence; **: determined by X-ray diffraction and Rietveld analysis using the Fullprof_suite package (Frontera *et al.*, 2003)

Table 2 : Cement compositions investigated experimentally (indicated by #, same numbers as in Figure 1) and by thermodynamic modeling (indicated by M).

		Weight fraction			Weight of raw materials(g)			Weight of anhydrous phases and water (g)				
		Clinker	Anhydrite	CaO	Clinker	Anhydrite	CaO	$C_4A_3\bar{S}$	C_2S	$C\bar{S}$	CaO	water
#3	M-1	0.800	0.050	0.150	4.000	0.250	0.750	2.172	1.164	0.266	0.758	30.000
	M-2	0.800	0.075	0.125	4.000	0.375	0.625	2.172	1.164	0.391	0.633	30.000
	M-3	0.800	0.100	0.100	4.000	0.500	0.500	2.172	1.164	0.516	0.508	30.000
#6	M-4	0.800	0.125	0.075	4.000	0.625	0.375	2.172	1.164	0.641	0.383	30.000
	M-5	0.800	0.150	0.050	4.000	0.750	0.250	2.172	1.164	0.766	0.258	30.000
	M-6	0.800	0.175	0.025	4.000	0.875	0.125	2.172	1.164	0.891	0.133	30.000
#2	M-7	0.800	0.200	0.000	4.000	1.000	0.000	2.172	1.164	1.016	0.008	30.000
	M-8	0.825	0.050	0.125	4.125	0.250	0.625	2.240	1.200	0.267	0.633	30.000
#10	M-9	0.825	0.075	0.100	4.125	0.375	0.500	2.240	1.200	0.392	0.508	30.000
	M-10	0.825	0.100	0.075	4.125	0.500	0.375	2.240	1.200	0.517	0.383	30.000
	M-11	0.825	0.125	0.050	4.125	0.625	0.250	2.240	1.200	0.642	0.258	30.000
#9	M-12	0.825	0.150	0.025	4.125	0.750	0.125	2.240	1.200	0.767	0.133	30.000
	M-13	0.825	0.175	0.000	4.125	0.875	0.000	2.240	1.200	0.892	0.008	30.000
	M-14	0.850	0.050	0.100	4.250	0.250	0.500	2.308	1.237	0.267	0.509	30.000
	M-15	0.850	0.075	0.075	4.250	0.375	0.375	2.308	1.237	0.392	0.384	30.000
#7	M-16	0.850	0.100	0.050	4.250	0.500	0.250	2.308	1.237	0.517	0.259	30.000
	M-17	0.850	0.125	0.025	4.250	0.625	0.125	2.308	1.237	0.642	0.134	30.000
	M-18	0.850	0.150	0.000	4.250	0.750	0.000	2.308	1.237	0.767	0.009	30.000
#5	M-19	0.875	0.050	0.075	4.375	0.250	0.375	2.376	1.273	0.268	0.384	30.000
	M-20	0.875	0.075	0.050	4.375	0.375	0.250	2.376	1.273	0.393	0.259	30.000
	M-21	0.875	0.100	0.025	4.375	0.500	0.125	2.376	1.273	0.518	0.134	30.000
#4	M-22	0.875	0.125	0.000	4.375	0.625	0.000	2.376	1.273	0.643	0.009	30.000
	M-23	0.900	0.050	0.050	4.500	0.250	0.250	2.444	1.310	0.268	0.259	30.000
#8	M-24	0.900	0.075	0.025	4.500	0.375	0.125	2.444	1.310	0.393	0.134	30.000
	M-25	0.900	0.100	0.000	4.500	0.500	0.000	2.444	1.310	0.518	0.009	30.000
	M-26	0.925	0.050	0.025	4.625	0.250	0.125	2.511	1.346	0.269	0.134	30.000
	M-27	0.925	0.075	0.000	4.625	0.375	0.000	2.511	1.346	0.394	0.009	30.000
#1	M-28	0.950	0.050	0.000	4.750	0.250	0.000	2.579	1.382	0.269	0.010	30.000

Table 3 : Composition of cement pastes (for 1 L).

Reference	AN-06	AN-05	Reference	GY-06	GY-05
Clinker (g)	857.30	960.19	Clinker (g)	867.41	972.90
Anhydrite (g)	214.32	240.05	Gypse (g)	274.24	307.60
Demineralized water (g)	642.97	600.12	Demineralized water (g)	593.15	543.68
	w/c = 0.6	w/c = 0.5		w/c* = 0.6	w/c* = 0.5

* including water brought by gypsum.

Table 4: Dehydration temperatures (main weight losses) of some cement hydrates.

Mineral	Temperatures of main weight losses	Reference
Ettringite	127°C	(Berger, 2009)
Monosulfate	85°C, 129°C, 192°C, 292°C	(Berger, 2009)
$C_3A.1/2C\bar{S}.1/2CH.H_{10}$	100°C, 190°C, 300°C	(Wenda, 1984)
$C_3A.1/2C\bar{C}.1/2CH.H_{11}$	120	(Pöllmann, 1984)
Strätlingite	131, 181, 226	(Fleischer <i>et al.</i> , 1977)
Katoite	210 – 350°C	(Rivas-Mercury <i>et al.</i> , 2008)
AH ₃ gel	90-120	(Ukrainczyk <i>et al.</i> , 2007)
Aluminum hydroxide (poorly crystallized)	255	(Berger, 2009)
C-S-H	100-150	(Saika <i>et al.</i> , 2006)

Table 5: Influence of the cement composition on its water demand. Comparison of the bw/c ratios determined experimentally and calculated using thermodynamic modeling.

Cement composition	Experimental bw/c ratio	Calculated bw/c ratio
#1	0.53	0.49
#2	0.61	0.62
#3	0.35	0.44
#4	0.59	0.55
#5	0.44	0.44
#6	0.50	0.50
#7-1	0.51	0.50
#7-2	0.51	0.50
#7-3	0.52	0.50
#8	0.53	0.50
#9	0.57	0.56
#10	0.43	0.44

Table 6: Estimated model coefficients for the bw/c ratio.

Response	b₁	b₂	b₃	b₁₂	b₁₃	b₂₃	b₁₂₃
bw/c	0.469	-1.766	-1.110	3.675	0.465	10.259	-8.533

Table 7: Influence of the calcium sulfate source, w/c ratio and hydration time on the amount of bound water, normalized with respect to the initial mass of cement (bw/c), in the paste samples (curing at $25 \pm 1^\circ\text{C}$ in airtight polypropylene boxes).

Age of sample	AN-05	AN-06	GY-05	GY-06
	Anhydrite w/c = 0.5	Anhydrite w/c = 0.6	Gypsum w/c* = 0.5	Gypsum w/c* = 0.6
1 d	0.35	0.38	0.34	0.38
7 d	0.37	0.41	0.34	0.38
23 d	0.37	0.43	0.35	0.39
90 d	0.40	0.48	0.39	0.43
Chemical water demand	0.62	0.62	0.62	0.62

* w = mixing water + water brought by gypsum; c = mass of cement + mass of CaSO_4

Table 8: Assessment of the amounts of free and bound water in the 90 d-old paste samples (1 L) (curing at $25 \pm 1^\circ\text{C}$ in airtight polypropylene boxes).

Paste reference	AN-05	AN-06	GY-05	GY-06
	Anhydrite w/c = 0.5	Anhydrite w/c = 0.6	Gypsum w/c = 0.5	Gypsum w/c = 0.6
Total water (g)	600.1	643.0	543.7	593.2
Bound water (g)	483.9	511.7	471.0	461.0
Free water (g)	116.3	131.3	137.0	189.5
Bound water (%)	80.6	79.6	77.5	70.9
Free water (%)	19.4	20.4	22.5	29.1

Figure 1: Experimental domain and selected design (as an example, the coordinates of point A corresponding to mix #3 are given by the dotted lines, i.e. Clinker fraction = 0.8, CaO fraction = 0.15, Anhydrite fraction = 0.05).

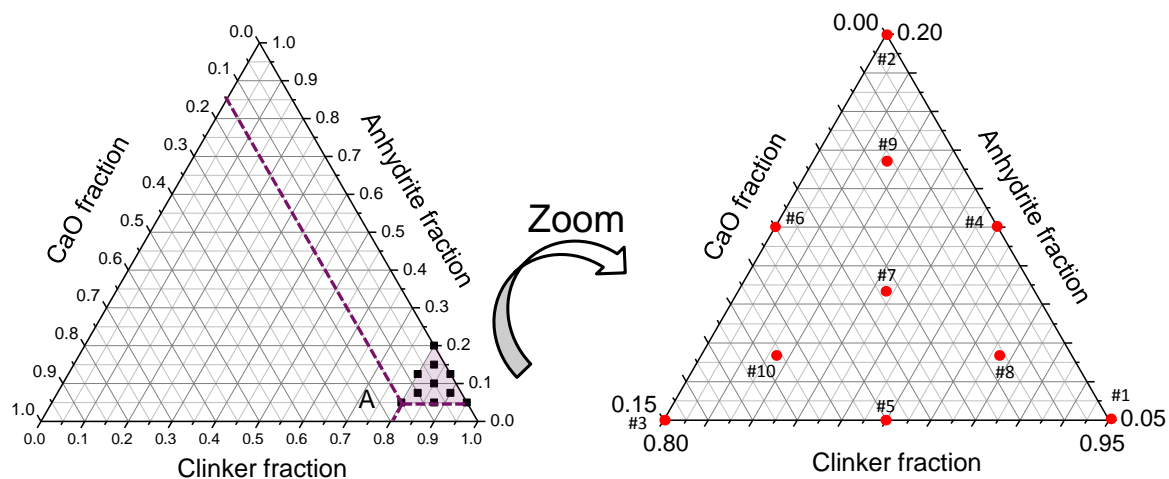


Figure 2: Diffraction patterns of the solid fractions of the cement suspensions after 1 month of stirring at ambient temperature (S: strätlingite, L: C₂S, E: ettringite, K: katoite, P: perovskite, M: monosulfate, Si: silicium).

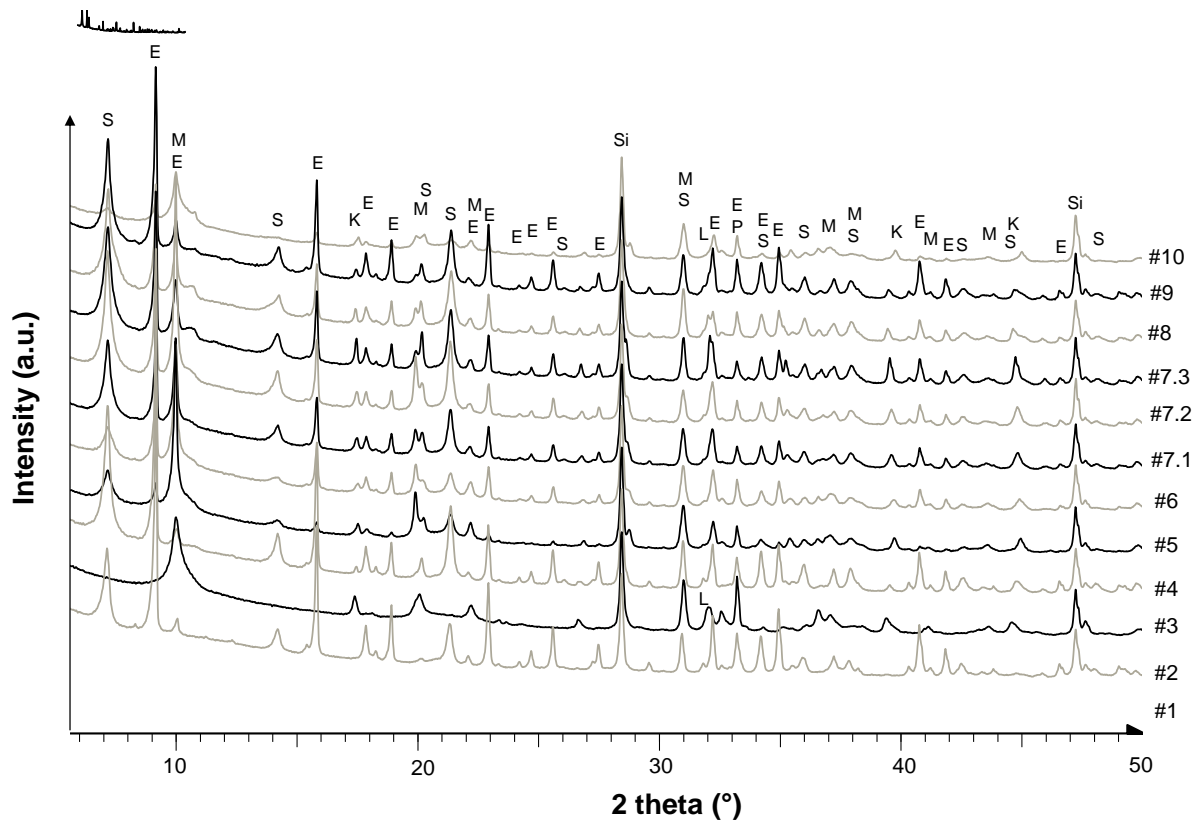


Figure 3: TGA analysis of the solid fractions of the suspensions after one month of stirring.

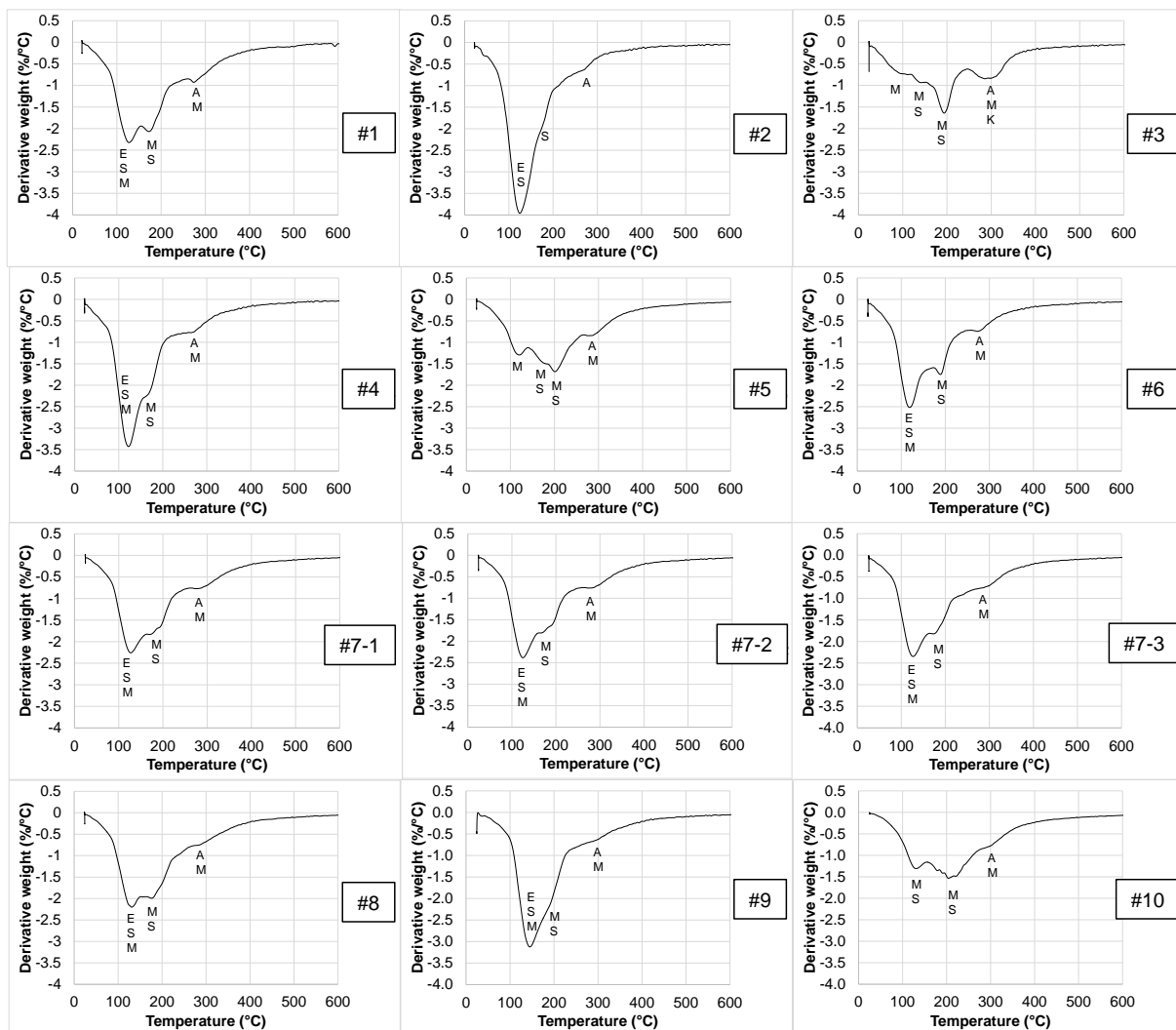


Figure 4: Influence of the initial composition of the cement on the phase assemblage formed at thermodynamic equilibrium once hydration is complete. The 3D plots show the calculated variation of the weights of hydrates (strätlingite, ettringite, monosulfate) formed by hydration of 5 g of cement.

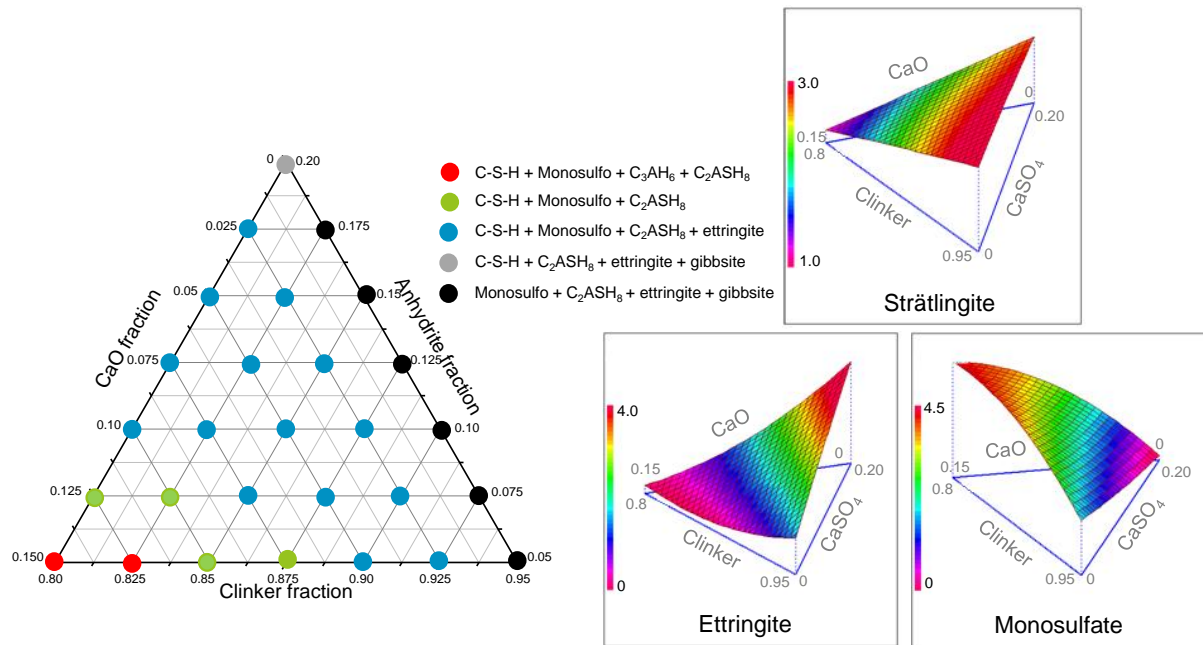


Figure 5: Influence of the cement composition on the amount of water bound by hydration. Comparison of the bw/c ratio after one month of stirring at ambient temperature (left) to the chemical water demand calculated by thermodynamic modeling (right).

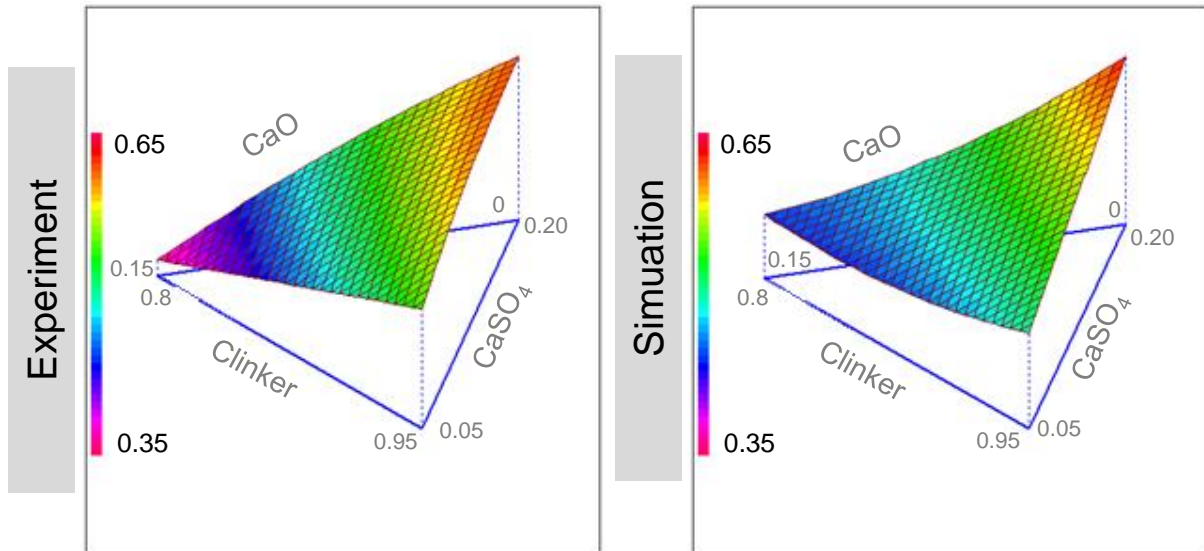


Figure 6: Evolution of the conductivity of demineralized water with additions of gypsum (left) or anhydrite (right).

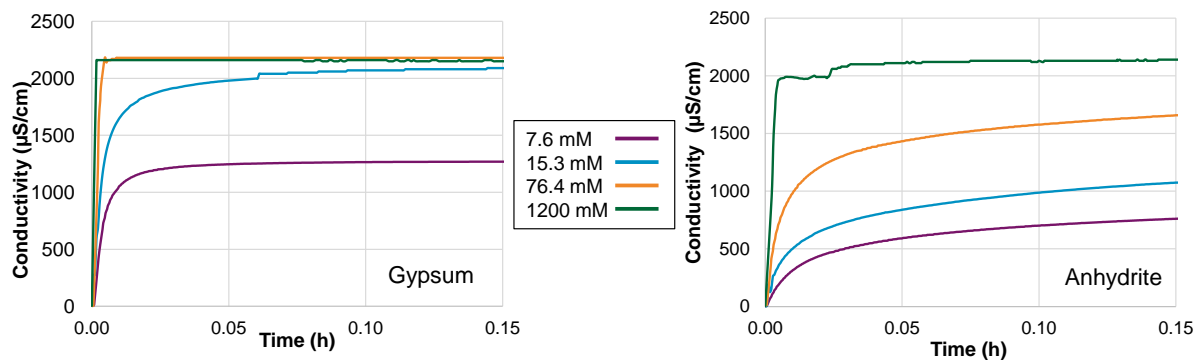


Figure 7: Influence of the calcium sulfate source and of the w/c ratio on the rate of hydration of CSAC pastes. Heat flow (left) and cumulative heat (right) recorded by isothermal calorimetry.

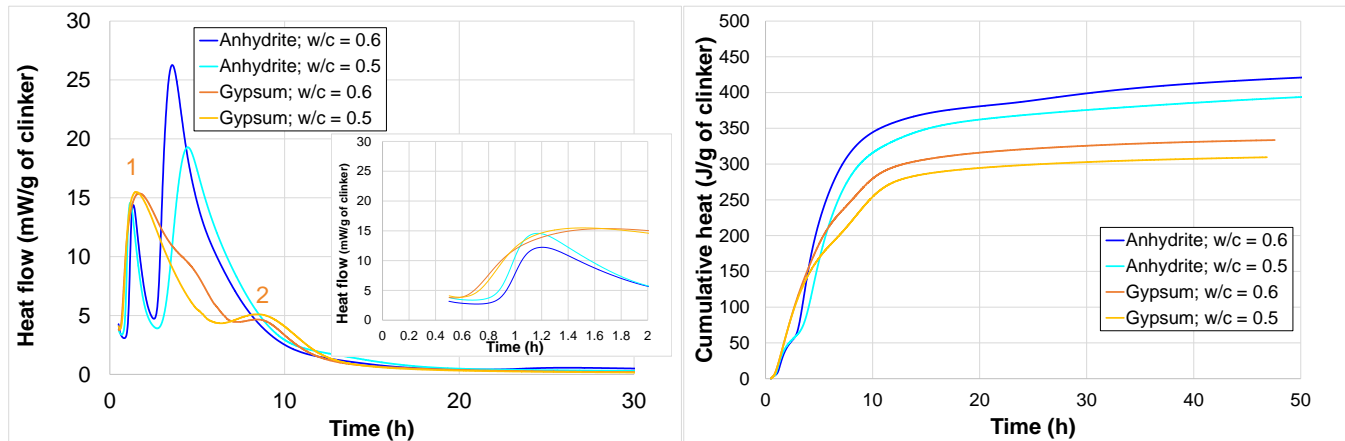


Figure 8: Evolution of the crystallized phases of the cement pastes prepared with anhydrite (w/c = 0.5 or 0.6) during hydration.

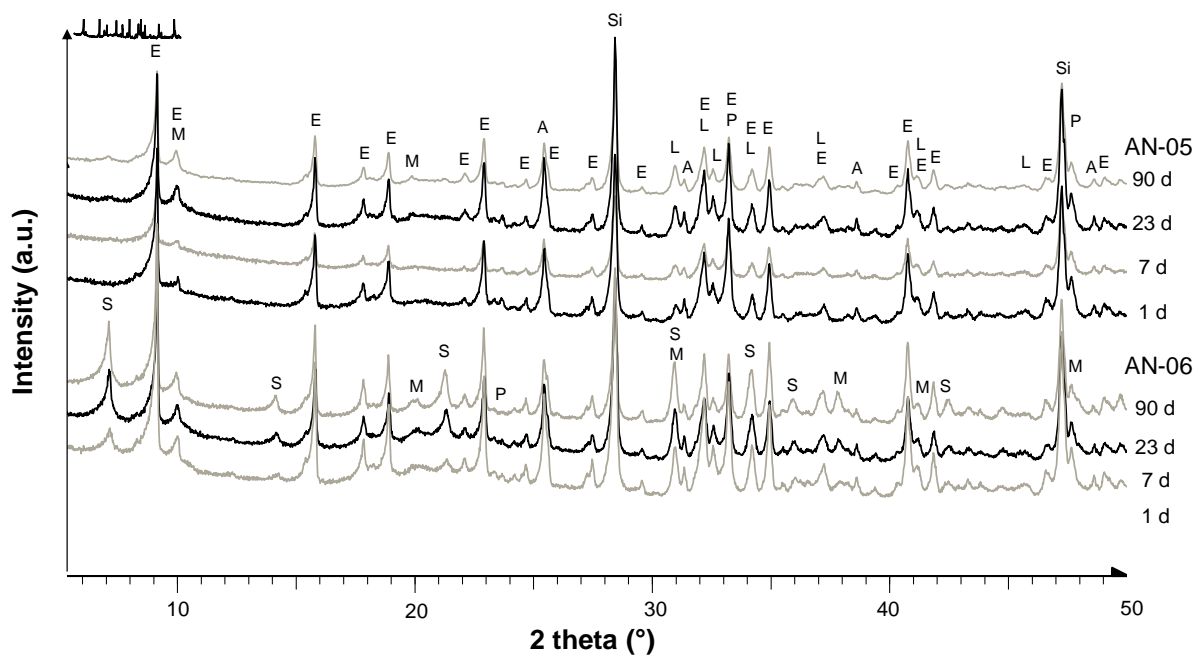


Figure 9: Evolution of the crystallized phases of the cement pastes prepared with gypsum ($w/c = 0.5$ or 0.6) during hydration.

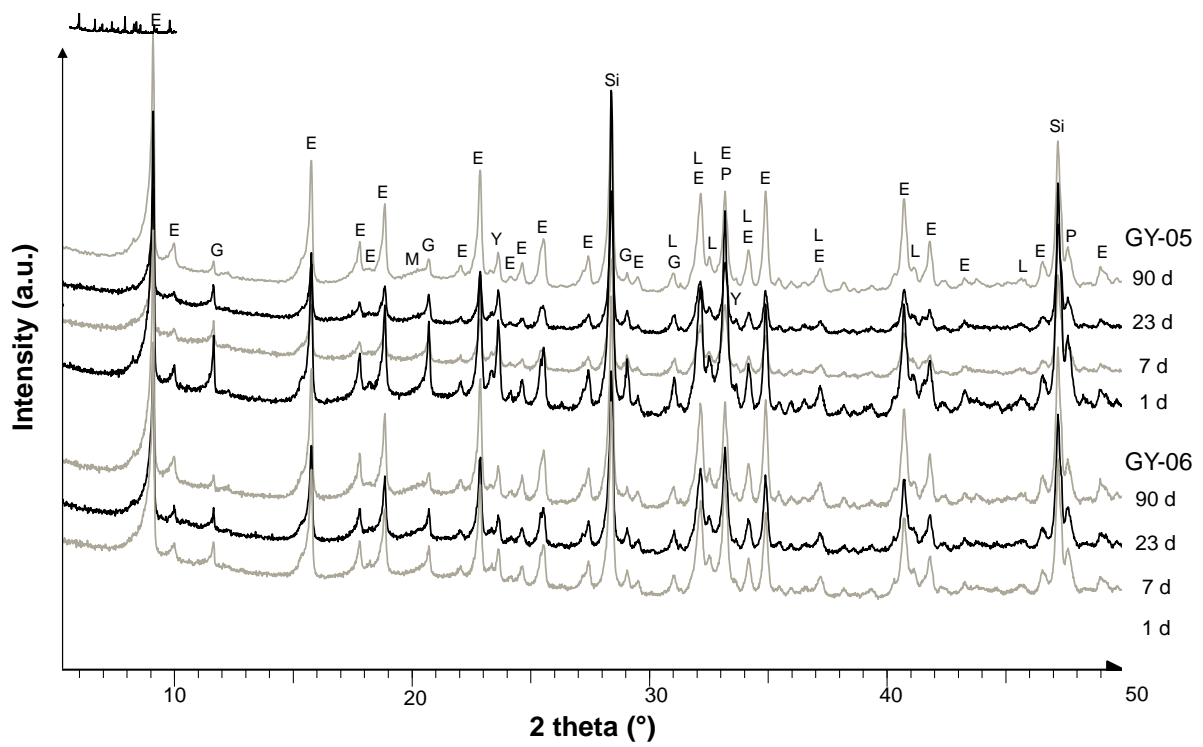


Figure 10: TGA analysis of the cement pastes after 1 d to 90 d of hydration.

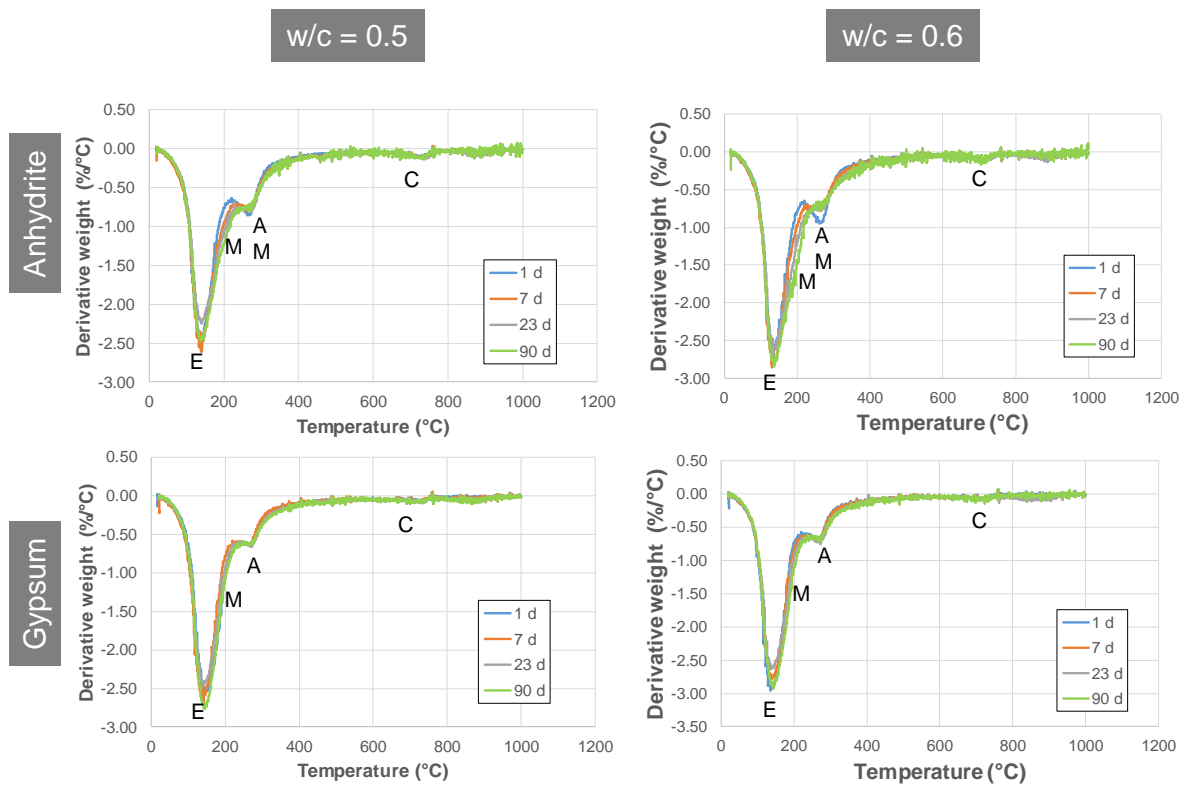


Figure 11: SEM observation (backscattered electrons) of a polished section of 1 d-old cement pastes prepared with anhydrite (left – 1: residual clinker; 2: residual anhydrite, 3: microporous zone containing ettringite, 4: denser zone containing aluminum hydroxide) or gypsum (right – 1: residual clinker, 2: residual gypsum, 3: hydrates) ($w/c = 0.6$).

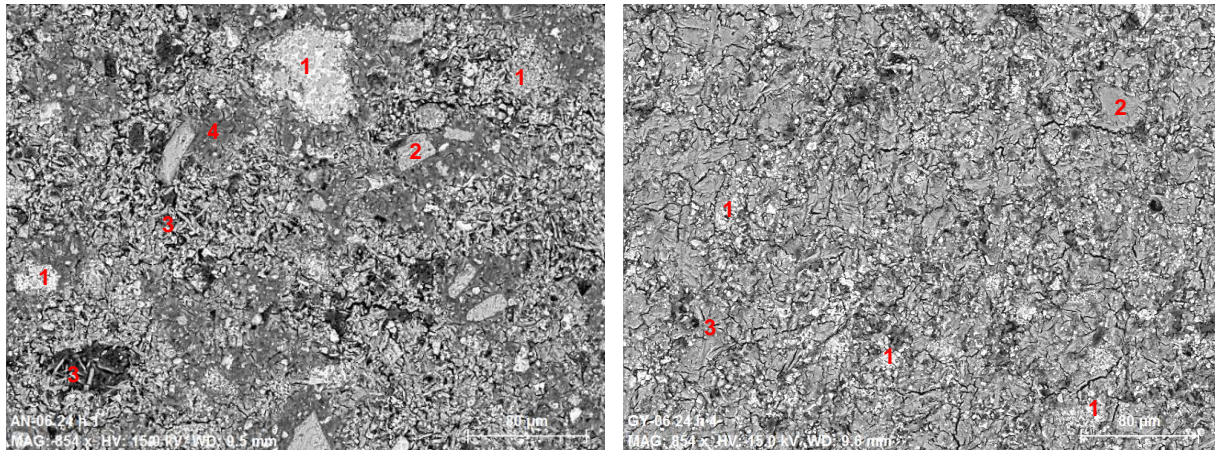


Figure 12: Length and mass variations of 4×4×16 cm specimens cured at room temperature in sealed bag or under water, and at 38°C and 100% R.H.

